Effect of Geometry on Heave Plate Hydrodynamics

Curtis J. Rusch*
University of Washington
Seattle, WA, USA

Thomas Boerner
CalWave/Hamburg University of Technology
Berkeley, CA, USA

Robert J. Cavagnaro
Applied Physics Lab - UW
Seattle, WA, USA

Benjamin Maurer
Applied Physics Lab - UW
Seattle, WA, USA

Norbert Hoffmann
Hamburg University of Technology
Hamburg, Germany

Brian Polagye
University of Washington
Seattle, WA, USA

*Corresponding author: curusch@uw.edu

1. INTRODUCTION

Heave plates provide the necessary reaction force for some point-absorbing wave energy converters. This reaction force is the result of inertia due to heave plate mass and added mass from water surrounding the plate, as well as viscous drag. The magnitude and phase of these forces is still not well understood for a broad range of shapes. This work examines how parameters, such as porosity, hole size, and perimeter, affects hydrodynamics. This information will aid in the design of future heave plates, allowing for a more targeted approach to their design and selection.

2. PRIOR WORK

The ocean engineering community has studied the hydrodynamics of oscillating bodies for many decades. Morison et al. [1] provides one of the earliest contributions to the field, studying the oscillating force experienced by piles in waves and formulating the widely used Morison equation. Studying flat plates in oscillating flow, Keulegan and Carpenter identify a parameter that describes the ratio of hydrodynamic forces from water inertia and viscous effects of oscillating plates across scales, now referred to as the Keulegan-Carpenter (KC) number [2]. When used for oscillations of regular sinusoidal motion, the KC number can be expressed as:

$$KC = \frac{2\pi a}{D}, \tag{1}$$

where a is oscillation amplitude, and D is heave plate diameter.

Li et al. [3] provides a sweep of parameters, including edge shape, distance from the free surface, thickness-to-width ratio, porosity, hole size, and the effect of stacking plates. They conclude that added mass decreases across all KC numbers with increasing porosity, and that drag increases, predominantly at low KC number, with increasing porosity. Additionally, they find that hole size has almost no impact on the total hydrodynamic force.

Tao and Dray [4] also studied the effect of porosity on induced hydrodynamic forces of heave plates. They noted a decreasing trend in added mass with increasing porosity. From their results, drag appears to change little for porosities between 0 and 10%, with a slight decrease around a porosity of 20%. Garrido-Mendoza et al. [5] studied the effect of distance from the seabed to mean plate position, showing that distances greater than a diameter sufficiently approximate deep water.

More recently, Rusch et al. [6] confirmed that the hydrodynamics of 3D, asymmetric heave plates scale with the KC number, much in the same way as flat plates, and showed that asymmetric heave plates have mildly asymmetric hydrodynamics in the heave direction. Similarly, Brown et al. [7] compared a 2D and 3D shape, with and without a large central opening. This showed a decreased hydrodynamic force when the central opening is present, in line with prior work.

Work by Mundon et al. [8] displays the importance of this research for the wave energy industry. Investigating small scale hydrodynamics of Oscilla Power's novel, 3D heave plate, they show that drag and added mass coefficients collapse at larger KC numbers, with some Reynolds number dependence for tests with the lowest velocities. They also present comparisons with CFD, showing promising agreement in heave.

3. METHODS

This study assesses the hydrodynamic forces generated by thirteen different heave plates, all shown in Figure 1. Three geometric groups are tested: squares, rectangles, and "so-called" Newman shapes. These groups contain two heave plate types: solid and perforated. The area enclosed by the perimeter of each heave plate is identical ($0.16\ m^2$). The perforated plates have a con-

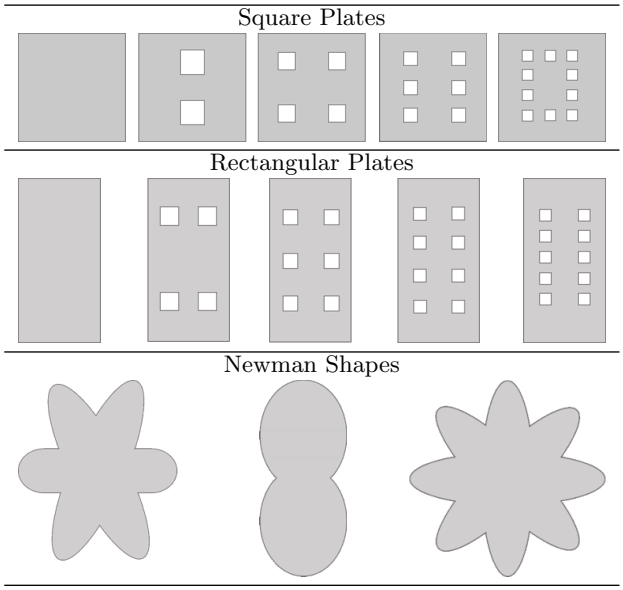

Figure 1: Heave plates used in testing

stant solidity of 90%, but varied hole sizes. Of the five square plates, one is solid and the remaining four have 2, 4, 6, and 10 holes, as shown in Figure 1. Five rectangular plates, with a 2:1 aspect ratio, are also tested, with 0, 4, 6, 8, and 10 holes. The Newman shapes, whose geometries are based on a weighted sum of sines and cosines, are inspired by work to amplify surface waves conducted by J. N. Newman [9]. The last row of Figure 1 shows the three Newman shapes, which we denote A, B, and C, from left to right. These shapes allow for large changes in perimeter while maintaining constant area.

3.1 Experimental Testing

The heave plates are tested using the "Oscillator", a vertically oriented linear actuator placed at the edge of a dock. Using this actuator, described in [6, 7], each rigidly connected heave plate is forced vertically through the water in regular sinusoidal motion of variable frequency and amplitude. The Oscillator uses feedback position control, and data output includes carriage position and force recorded at the actuator. Total force induced in the heave direction is measured using a 2200 N rated S-beam load cell, with a noise floor of about 3 N, and the data acquisition system records force and position at 2 kHz. The water at the side of the dock is open to recreational boating and small commercial shipping traffic, but the occasional wakes that reach the dock are of minimal size, and are observed to have negligible impact on the data. The distance from water surface to mean plate position is 1.02 m, with a total water depth of just over 3 meters and effectively unbounded sides. Both surfaces are more than two diameters away from mean plate position, indicating negligible surface effects [5].

The suite of tests is the same for each plate, covering periods from 0.5 - 4 s, and KC numbers from 0.14 - 5.59. Critical to this analysis, in Eqn 1, we use an effective diameter, D, defined as the diameter of a circle with area equal to that of the area enclosed by a heave plate's perimeter (as defined in [6]). This definition results in an equal effective diameter for all heave plates tested.

Table 1: Maximum cycle speed (cm/s) for each conducted test.

	Period (s)			
KC	0.5	1.0	2.0	4.0
0.14	12.6			
0.21	18.8			
0.28	25.1	12.6		
0.35	31.4	15.7		
0.52	47.1	23.6		
0.7		31.4	15.7	
1.4		62.8	31.4	
2.09			47.1	
2.79			62.8	31.4
4.19				47.1
5.59				62.8

Sinusoids producing higher forces (larger amplitude and higher frequency) improve the signal to noise ratio, but are limited by the maximum Oscillator speed of about 0.65 m/s. Table 1 shows the maximum speeds reached for each test. As the KC number increases, a larger oscillation period is required due to the maximum speed restriction. For each new period, an overlap in KC number with other periods allows for analysis of frequency dependence.

These heave plates are candidates for field-testing with a small wave energy converter deployed in a scaled wave environment, with expected KC numbers below one. Therefore, as seen in Table 1, experimental assessment focuses on KC numbers in this range, with a more limited set of experiments to explore hydrodynamic responses to larger oscillation amplitudes. This parameter space is designed to thoroughly examine everyday conditions, while providing data to assess the response in larger sea states.

3.2 Data Analysis

To asses hydrodynamic forces on the plates, forces induced by other physical phenomena, such as component inertia (static mass x acceleration), static weight, and buoyancy, are removed as:

$$F_{hydro} = F_{measured} - W + F_b - F_i, \qquad (2)$$

where F_{hydro} is the hydrodynamic force, $F_{measured}$ is the force recorded by the load cell, W is the weight of all components, F_b is the buoyancy of all submerged components, and F_i is the force resulting from component inertia.

The Morison equation is then used to decompose this hydrodynamic force into the viscous and added mass components using the known heave plate velocity and acceleration:

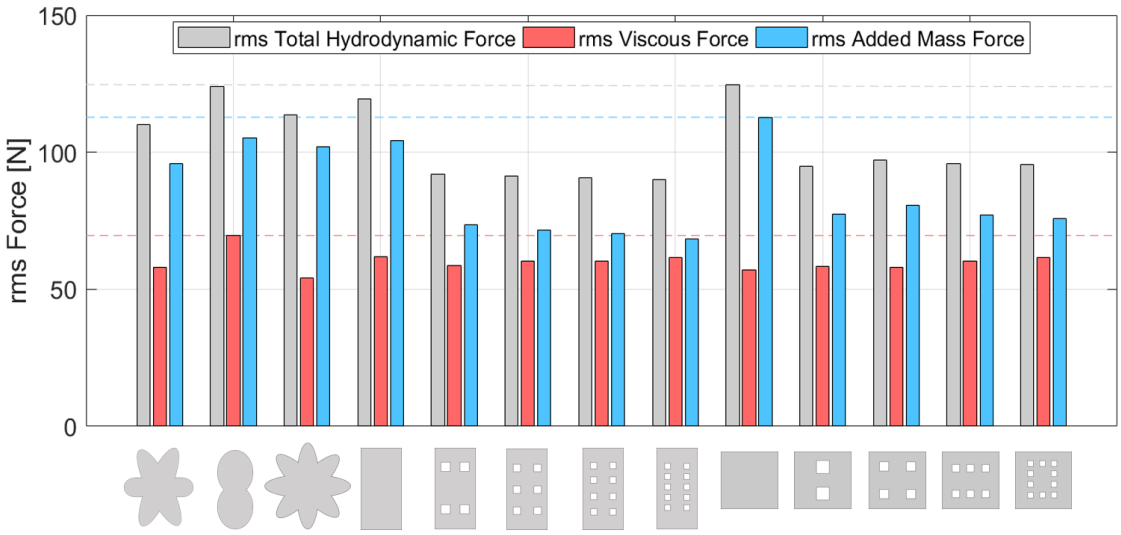

Figure 2: Plot of rms total hydrodynamic force (based on the force reconstruction) for each plate, alongside the rms viscous and added mass forces, when $KC = 0.35$ and $T = 0.5\ s$.

$$\begin{bmatrix} F_{hyrdo}(t_1) \\ F_{hydro}(t_2) \\ \vdots \end{bmatrix} = A \begin{bmatrix} \dot{z}_1|\dot{z}_1| \\ \dot{z}_2|\dot{z}_2| \\ \vdots \end{bmatrix} + B \begin{bmatrix} \ddot{z}_1 \\ \ddot{z}_2 \\ \vdots \end{bmatrix}. \quad (3)$$

Using a least squares solution, we can solve for the constants, A and B. From these constants, we define our coefficient of drag as

$$C_d \equiv \frac{F_d}{\frac{1}{8}\rho\pi D^2 \dot{z}|\dot{z}|} = \frac{A}{\frac{1}{8}\rho\pi D^2}, \quad (4)$$

and our coefficient of added mass as

$$C_a \equiv \frac{F_a}{\frac{1}{6}\rho\pi D^3 \ddot{z}} = \frac{B}{\frac{1}{6}\rho\pi D^3}. \quad (5)$$

F_d and F_a represent the forces resulting from drag and added mass, respectively, and ρ is the density of fresh water (1000 kg/m^3). Coefficients are calculated over a time window of exactly one period. The window is then shifted one data point forward and a new solution is found, until the end of the time series is reached. The coefficients of drag and added mass are represented by their median, and we use the 25^{th} and 75^{th} percentiles to quantify variation.

As a final step, we reconstruct an approximation of the viscous, added mass, and total hydrodynamic forces. After solving Eqn. 3, multiplication of A by the time series $\dot{z}(t)|\dot{z}(t)|$ yields an approximation of the time resolved viscous force. Similarly, $B * \ddot{z}(t)$ yields an approximation of the time resolved added mass force. The sum of viscous and added mass terms yields an approximation to the time resolved total hydrodynamic force, which closely matches the initial hydrodynamic force term. We use the root mean square (rms) of the time series for each of these forces as a way to compare the relative contribution of viscous and added mass forces to the total hydrodynamic force.

4. RESULTS AND DISCUSSION

Figure 2 provides a summary of the balance of forces acting on the thirteen plates tested for a single KC number and period. The rms hydrodynamic force is not equal to the sum of the viscous and added mass forces because those two forces are out of phase.

As shown in Figure 2, the solid square plate produced the largest total hydrodynamic force, as well as the largest added mass force. Additionally, the forces decrease dramatically when holes are added, in line with prior results [3, 7], with little change as the number of holes increases (porosity held constant). Newman shape B has a force breakdown that is similar to the solid rectangle, likely due to the similarity in shape between the two. Figure 2 emphasizes the dominance of added mass forces at low KC number in solid plates, and displays how the added mass and viscous forces are nearly equivalent for plates with holes.

Trends in the hydrodynamics for all tests are shown in Figure 3. Coefficients of drag and added mass are dependent on the KC number, and independent of oscillation frequency. The coefficient of drag is highly nonlinear for KC numbers less than one, and asymptotes to a constant value at higher KC numbers. In contrast, the coefficients of added mass follow a linear, increasing trend across the range of KC numbers tested. Additionally, added mass variability increases for tests at larger KC numbers. We hypothesize that this may be a result of unpredictable vortex detachment at high KC numbers. We add that, at low KC numbers, the vortices are destroyed before they detach in a predictable manner, as the heave plate reverses direction.

Comparisons between the three plate groups are also instructive. Figure 3 shows that at high KC numbers, drag coefficients are nearly constant with geometry, with slight differences at small KC numbers. At low KC numbers, the square plate has the highest added mass coefficient, while the Newman plate the smallest. For KC numbers greater than one, the Newman plate overtakes

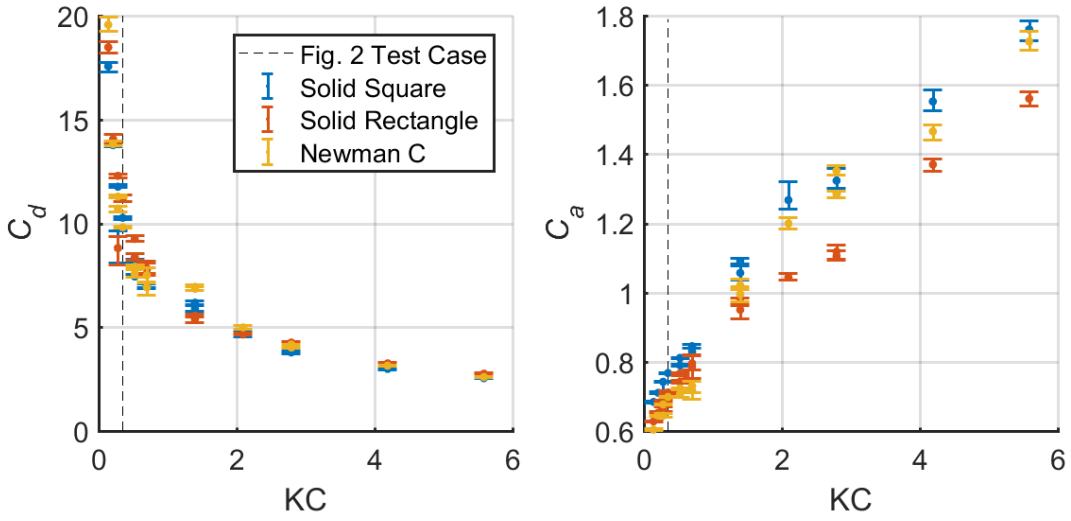

Figure 3: Calculated coefficients of drag and added mass for the tests with the solid square (blue), the solid rectangle (red), and Newman plate C (yellow). The error bars represent the 25th and 75th percentile, with respect to the median value, and the dashed line shows the case depicted in Figure 2.

the rectangle, and even approaches the added mass of the square. We believe that, at low KC number, the added mass may be governed by some cross-plate distance. For smaller cross-plate distances, plates may exhibit lower added mass coefficients, while larger distances would result in higher coefficients. This makes continuous, symmetric shapes (such as the square) more desirable for wave energy conversion. For high KC numbers, small features, such as the concave corners of Newman shape C, may become engulfed in the boundary layer of the plate, changing the effective cross-plate distance. This leads to strikingly similar hydrodynamics between different radially symmetric shapes at high KC numbers, despite their differences at low KC number.

Not shown in the plots, radially symmetric plates tend to exhibit greater stability in the surge and sway directions than asymmetric plates. For example, on some oscillations, the rectangular plates induce a slight side-to-side vibration, a phenomenon not seen in the squares. Additionally, Newman plates A and B, which are less radially symmetric, experience similar vibration, while the more radially symmetric plate C is more stable.

5. SUMMARY AND NEXT STEPS

It was shown that, at low KC numbers, added mass is the dominant component of the total hydrodynamic force, but is significantly reduced when porosity is introduced. Drag shows little change between all of the plates tested. This motivates the need to better understand added mass. We will conduct more analysis in the coming months regarding the specific effects of perimeter, hole size, and cross-plate dimensions as they pertain to the hydrodynamics. Further, we will conduct numerical simulation, using Boundary Element Method and Computational Fluid Dynamics approaches, to assess the usefulness of computer modeling in heave plate design. We expect to develop guidelines for a broad set of characteristics and how they effect the hydrodynamics of heave plates, allowing for a more methodical design iteration process to find optimal heave plate shapes for wave energy conversion.

6. ACKNOWLEDGEMENTS

The authors would like to thank NAVFAC for the funding that allowed for this strong collaboration between CalWave and the University of Washington. We would like to thank Nigel Kojimoto and Bryan Murray of CalWave for their help with Oscillator testing, and Adam Brown for his initial work building the Oscillator.

7. REFERENCES

[1] Morison, J. R., Johnson, J. W., Schaaf, S. A., and O'Brien, M. P., 1950. "The Force Exerted by Surface Waves on Piles". *Journal of Petroleum Technology,* ***2***(5), pp. 149–154.

[2] Keulegan, G. H., and Carpenter, L. H., 1958. "Forces on Cylinders and Plates in an Oscillating Fluid". *Journal of Research of the National Bureau of Standards,* ***60***(5).

[3] Li, J., Liu, S., Zhao, M., and Teng, B., 2013. "Experimental investigation of the hydrodynamic characteristics of heave plates using forced oscillation". *Ocean Engineering,* ***66***, pp. 82–91.

[4] Tao, L., and Dray, D., 2008. "Hydrodynamic performance of solid and porous heave plates". *Ocean Engineering,* ***35***(10), pp. 1006–1014.

[5] Garrido-Mendoza, C. a., Thiagarajan, K. P., Souto-Iglesias, A., Colagrossi, A., and Bouscasse, B., 2015. "Computation of flow features and hydrodynamic coefficients around heave plates oscillating near a seabed". *Journal of Fluids and Structures,* ***59***, pp. 406–431.

[6] Rusch, C. J., Maurer, B. D., Mundon, T. R., Stewart, A., and Polagye, B., 2017. "Hydrodynamics and Scaling of Heave Plates for Point Absorbing Wave Energy Converters". In Proc of 12th European Wave and Tidal Energy Conference, pp. 1–8.

[7] Brown, A., Thomson, J., and Rusch, C., 2017. "Hydrodynamic Coefficients of Heave Plates , With Application to Wave Energy Conversion". *Journal of Ocean Engineering*, pp. 1–14.

[8] Mundon, T. R., Rosenberg, B. J., and Rij, J. V., 2017. "Reaction Body Hydrodynamics for a Multi-DOF". In Proc of 12th European Wave and Tidal Energy Conference, pp. 1–10.

[9] Newman, J. N., 2015. "Amplification of waves by submerged plates". In Proc of 30th IWWWFB, pp. 1–4.